




Numerical Study of Haline Convection in a Porous Domain with Application for Geothermal Systems

E. B. Soboleva^(✉) 

Ishlinsky Institute for Problems in Mechanics RAS, Moscow, Russia
soboleva@ipmnet.ru

Abstract. We study stochastic haline convection in a porous domain in a context of dissolved admixture transport problems in geothermal reservoirs. An isotropic homogeneous rectangular porous domain divided by a horizontal interior layer at lower porosity and permeability is considered. The upper boundary is assumed to be an admixture source leading to admixture diffusion into a volume and a development of gravity-driven haline convection. Numerical simulations of convective flows and mass transfer based on the continuity, Darcy's and admixture transport equations are performed. An influence of properties of interior layer on the convection structure and dynamic characteristics is investigated.

Keywords: Haline convection · Porous medium · Geophysical flows · Geothermal reservoir · Numerical simulation

1 Introduction

Many fields of human activity such as ecology, environmental management, mining industry need an information on admixture transport in groundwater. Salts dissolved in water move in soils and rocks in the Earth because of different reasons. Usually, the admixture transport is associated with forced or natural modes of convection and the last one is typically caused by the temperature and salinity gradients leading in the gravity field to a development of motions [1, 2]. In special cases, a growth of instability and motions arisen can be independent of gravity, for example, under the capillary pressure gradient [3–5] which, however, is not considered in the present study. Our study is devoted to natural gravity-driven convection associated with an admixture transport in a geothermal reservoir; the geothermal system is an alternative energy source using deep heat of Earth [6]. Similar problems on convective admixture transport are solved in the context of carbon capture and sequestration technologies [7, 8]. Groundwater with dissolved admixture is involved in thermal gravity-driven convection under the geothermal gradient resulted from the temperature rising in the direction to the hot Earth's core; this gradient is normally about 20–30K per each kilometer [9]. However, if salinity gradients are sufficiently high, haline (or as is also called, density-driven) convection can be more intensive in a comparison with thermal convection. Estimations show that, for a domain with the vertical size of 10 m, haline

convection is dominant starting with concentration differences in the domain of about $6 \cdot 10^{-4}$ [10]; parameters of water correspond to the real temperature and pressure in geothermal systems being of 500K and 150 atm, respectively. The concentration differences exceeding $6 \cdot 10^{-4}$ are observed in many real cases in which only haline convection can be taken into consideration disregarding thermal convection.

In this paper, we investigate numerically haline convection in a porous rectangular reservoir initially filled with pure motionless water. The constant admixture concentration is held at the upper boundary modeling a close location of salt source. An admixture diffuses into a volume forming a dense brine near the boundary which tries to fall so it gives rise to a development of haline convection. A domain consists of homogeneous isotropic porous medium divided by an interior horizontal layer at lower porosity and permeability. An effect of interior layer on the convection structure and dynamic characteristics is investigated. Here, we continue our study of haline convection in heterogeneous domains starting with [10, 11]. We consider wide interior layers, convective motions inside them and analyze spectrums of convection structures.

2 Mathematical Model and Numerical Method

We consider a homogeneous porous domain divided by a horizontal interior layer at different porosity and permeability (see Fig. 1). Initially, the domain is filled with pure motionless water. The constant admixture concentration is held at the upper boundary providing the admixture to diffuse into the volume. The solute density is lineally related to the admixture concentration so the dense brine is formed near the upper boundary. This brine tries to fall under the gravity force giving rise to a development of haline convective flows and mass transfer.

Haline convection in a porous domain is described by the governing equations, which are the continuity, Darcy’s and admixture transport equations. The governing equations can be written in a dimensionless form as follows

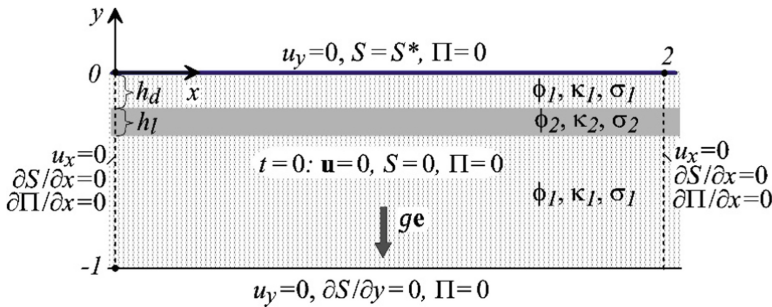


Fig. 1. Problem under study.

$$\nabla \cdot \mathbf{u} = 0 \quad (1)$$

$$\mathbf{u} = -Rd \kappa (\nabla \Pi - S \cdot \mathbf{e}) \quad (2)$$

$$\phi \frac{\partial S}{\partial t} + \mathbf{u} \cdot \nabla S = \nabla(\sigma \phi \nabla S) \quad (3)$$

The equations include $\mathbf{u} = \mathbf{U}H/D_c$, $\Pi = (P - P_{in})/(\alpha \rho_c^{sat} gH)$, and $S = \rho_c/\rho_c^{sat}$ to be the dimensionless filtration velocity, pressure, and admixture density, respectively. The velocity has the components: $\mathbf{u} = (u_x, u_y)$. Here, \mathbf{U} , P , P_{in} , ρ_c , ρ_c^{sat} , H , D_c , α , and g are the physical filtration velocity, actual and initial values of pressure, actual and maximal (corresponding to saturated brine) values of admixture density, height of domain, coefficient of molecular diffusion, salinity expansion coefficient, and module of gravity acceleration. The geometrical size and time are normalized by H and H^2/D_c , respectively. The initial and boundary conditions are given in Fig. 1.

Dimensionless parameters of the system are the Rayleigh-Darcy number Rd , relative permeability κ and coefficient of diffusion σ , as well as the porosity ϕ and the characteristic density S^* . From the definition

$$Rd = \frac{\alpha \rho_c^{sat} g k_1 H}{\mu_s D_c}, \kappa = k/k_1 \sigma = D/D_c \quad (4)$$

Subscripts “1” and “2” denote the main medium and interior layer, respectively. Superscripts “*” and “sat” denote the upper boundary and saturated brine. The conditions at the boundaries of interior layer are

$$\Pi_2 = \Pi_1, S_2 = S_1, u_{x2} = u_{x1} \kappa_2, u_{y2} = u_{y1}, w_{x2} = w_{x1} \kappa_2 \frac{\phi_1}{\phi_2}, w_{y2} = w_{y1} \frac{\phi_1}{\phi_2} \quad (5)$$

Here, w_x and w_y are the components of the fluid velocity $\mathbf{w} = (w_x, w_y) = \mathbf{u}/\phi$. Notice, a flow direction has to change when flow lines cross the interface that is resulted from the conditions (5).

Haline convection is simulated at parameters corresponding to real geological conditions: $\rho_0 = 842.5 \text{ kg m}^{-3}$, $\mu_s = 1.212 \cdot 10^{-4} \text{ Pa s}$, $c^{sat} = 0.3417$, $D_c = 3 \cdot 10^{-9} \text{ m}^2 \text{ s}^{-1}$, $\alpha = 0.815$. We put $\phi_l = 0.2$, $k_l = 1.0 \cdot 10^{-13} \text{ m}^2$, $D_l = 1.58 \cdot 10^{-9} \text{ m}^2 \text{ s}^{-1}$, $\phi_2 = 0.1$, $\kappa_2 = 1.0 \cdot 10^{-14} \text{ m}^2$, $D_2 = 1.19 \cdot 10^{-9} \text{ m}^2 \text{ s}^{-1}$. The height of domain is $H = 25 \text{ m}$, the distance from the upper boundary to the interior layer is $H_d = 1.25 \text{ m}$. The layer width H_l varies. The appropriate dimensionless quantities are $Rd = 2.19 \cdot 10^4$, $\kappa_l = 1$, $\sigma_l = 0.525$, $\kappa_2 = 0.1$, $\sigma_2 = 0.398$, $h_d = 0.05$. The dimensionless layer width is $h_l = 0$; 0.032; 0.11. We put admixture concentration at the top $c^* = 0.04$ that is equivalent to the dimensionless density $S^* = \frac{(1-\alpha c^{sat})c^*}{c^{sat}(1-\alpha c^*)} = 0.0873$. The aspect ratio of considered domain equals to 2.

Simulations are performed with the use of 2D finite-difference numerical code employed during several years to the problems of underground haline convection [10, 12–14]. The complicated mathematical model and last version of the code including tests are described in [8]. To obtain accurate numerical results we use very fine space grids up to 5000×2500 .

3 Results and Discussion

An admixture diffuses from the upper boundary to the volume so brine locating nearby is denser than pure water under this brine. Brine is unstable in the gravity field and tries to fall that leads to developing haline gravity-driven convection which is stochastic at considered parameters. The evolution of convective flows in a domain containing an interior layer at the width $H_l = 0.8$ m (or $h_l = 0.032$ in dimensionless form) is shown in Fig. 2. The interior layer is displayed in Figs. 2 and 4 with gray color. In the initial stage, brine fingers travelling from the upper boundary and filling the space above the interior layer completely occur (Fig. 2(a)). The layer passes an admixture difficultly because the permeability is lowered ten times comparing with a main medium. When an admixture reaches the layer, the maximal fluid velocity $|\mathbf{W}_{max}|$ characterizing the intensity of motions falls comparing with the case of no layer; the fluid velocity is defined as $\mathbf{W} = \mathbf{U}/\phi$. This trend is exhibited in Fig. 3: the curve 2 deviates from the curve 1 corresponding to the case of no layer and goes to bottom starting from $t \approx 400$ days. In the time period $t \approx 400$ –800 days, an admixture is transported throughout the layer by forced mode of convection. The motions of fluid in the layer are downward everywhere and the velocity is lowered due to the conservation law: no fluid comes to the space above the interior layer. Later, we observe crucial changing in the convection pattern that is resulted from convection in the layer to transform to natural. Some pure water starts to rise from the space below the layer, cross the layer and fill the space above the layer leaved by brine. Rising fingers of pure water split brine above the layer into a set of roughly periodic “brine balls” (Figs. 2(b–d)). This stage is characterized by an intensification of motions as an inflow of pure water makes up for an outflow of brine. As visible in Fig. 3, the velocity $|\mathbf{W}_{max}|$ increases starting from $t \approx 800$ days and even exceeds the appropriate value in a domain with no layer after $t \approx 2000$ days. The convection pattern in a domain as a whole is rearranged with time as well. We see small brine fingers travelling below the interior layer in the initial stage (Fig. 2(a)) which later merge and are located less often (Fig. 2(b)). To the time $t \approx 2550$ days and later, the brine fingers resemble jets taking off the layer (Fig. 2(c, d)).

For a comparison, a domain with a wider interior layer at $H_l = 2.75$ m (or $h_l = 0.11$ in dimensionless form) is considered. Convection patterns are shown in Fig. 4. The main features of convection evolution is the same as at $H_l = 0.8$ m discussed early. Initially, an admixture fills the space above the layer completely that is associated with a forced mode of convection in the layer (Fig. 4(a)). Later, fluid motions here are rearranged, some extended zones of pure water appear (Fig. 4(b, c)) so that pure water

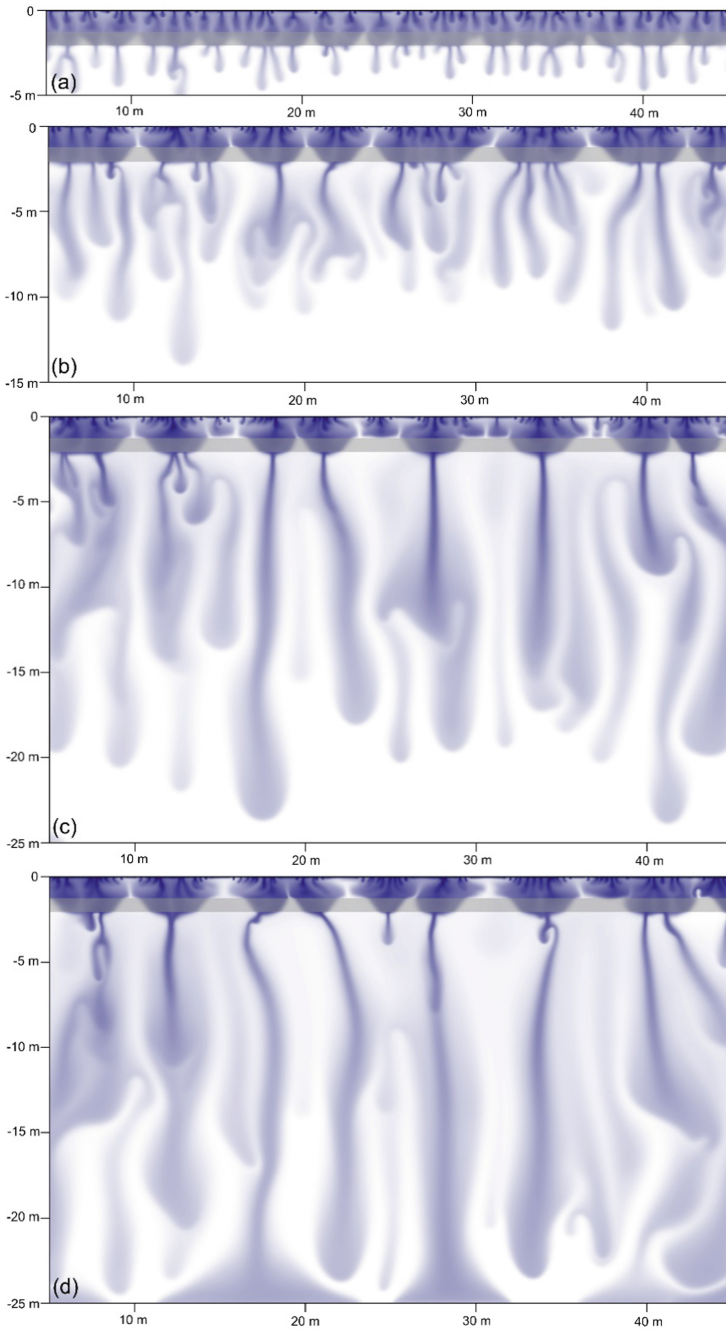


Fig. 2. Concentration field in a domain containing an interior layer at the width $H_l = 0.8$ m at times $t = 675$ (a), 1500 (b), 2550 (c), 3150 days (d).

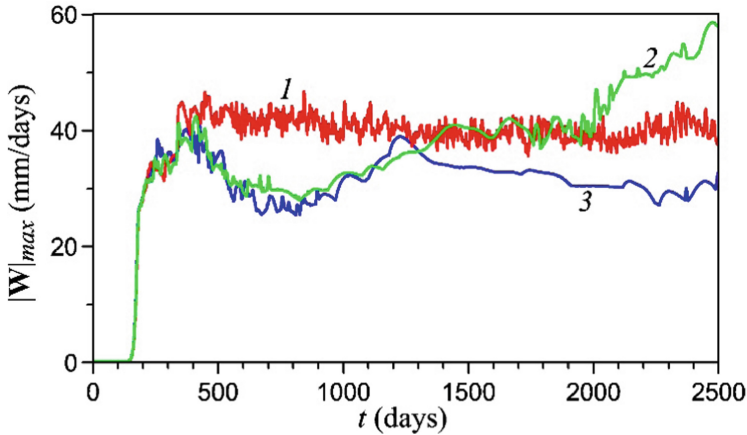


Fig. 3. Maximal fluid velocity $|\mathbf{W}_{max}|$ depending on the time in a domain without an interior layer (1) and containing the interior layer with the width $H_l = 0.8$ (2), 2.75 m (3).

starts to rise to the space above the layer (Fig. 4(d)). That rearranging is associated with transition to a natural mode of convection in the layer and formation of roughly periodic structure of “brine balls” above it (Fig. 4(d)). However, rearranging of motions takes a longer time as more fluid fills a wider layer. We see in Fig. 3 for the velocity $|\mathbf{W}_{max}|$, that the curves 3 and 2 corresponding to $H_l = 2.75$ m and $H_l = 0.8$ m behave similarly up to $t \approx 1300$ days. Then, the magnitudes of $|\mathbf{W}_{max}|$ become lower at $H_l = 2.75$ m than at $H_l = 0.8$ m because the natural convection does not manage to develop in the first case whereas it develops in the second case. The scale of “brine balls” is bigger in the first case that is clear from a comparison of Figs. 4(d) and 2(d). Maybe, “brine balls” in the first case will become smaller during further evolution, however we believe they average size to remain bigger then the size of “balls” in the second case. Each big “brine ball” corresponding to the case of $H_l = 2.75$ m, perhaps, will generate, in a very long time, a single jet falling down (similar to that in Fig. 2(d)), however, we do not continue numerical simulation to such time because an admixture reaches the lower boundary and accumulate nearby.

The case of domain with the interior layer at $H_l = 2.75$ m is considered. To exhibit how motions in an interior layer effect the convection structure above it, the horizontal density distributions $S_1(x) = S(x, -0.025)$ and $S_2(x) = S(x, -0.100)$ are analyzed. The function $S_1(x)$ is taken at the level $y = -0.025$ or, in dimensional variables, at 0.625 m below the upper boundary that is along the central line of space between the upper boundary and interior layer. The function $S_2(x)$ is taken at the level $y = -0.100$ to be at 2.50 m below the upper boundary and coincide with the central line of interior layer. So, $S_1(x)$ characterizes the density distribution in the space above the interior layer whereas $S_2(x)$ does it in the layer. We approximate the functions $S_1(x)$ and $S_2(x)$ with

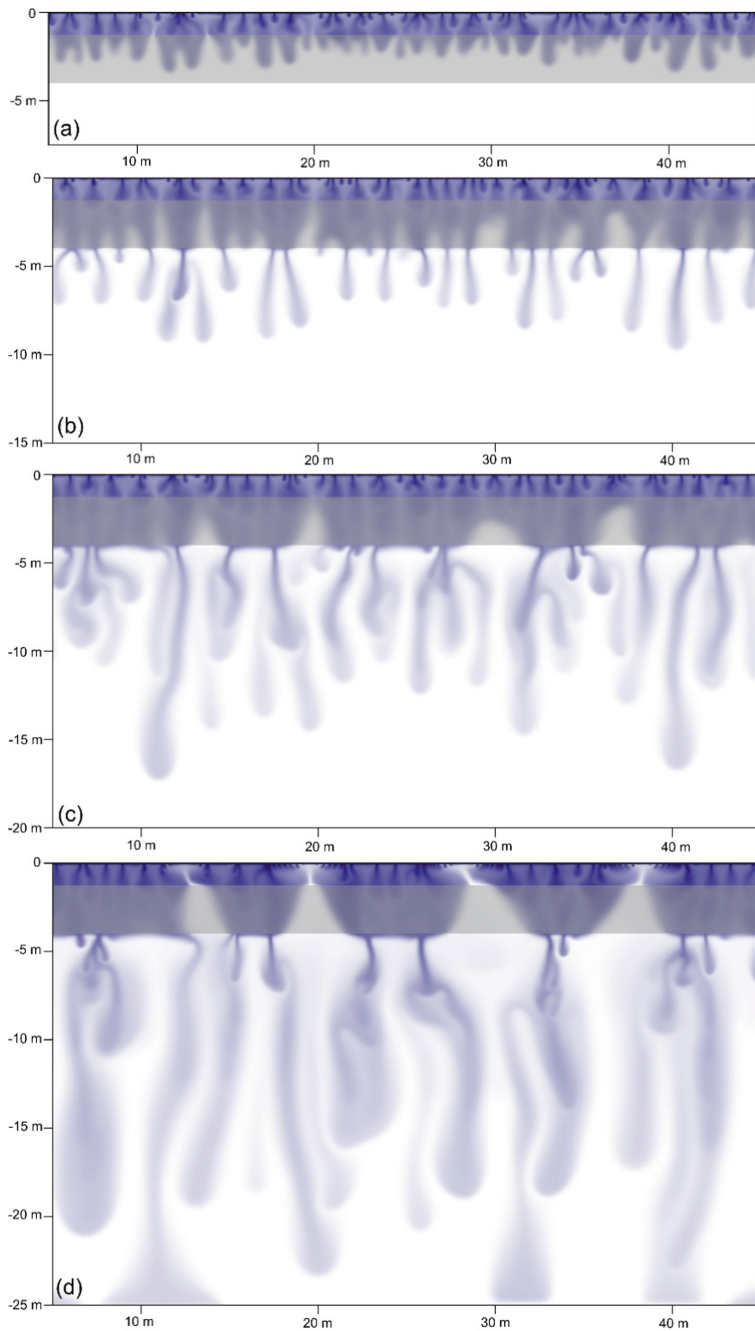


Fig. 4. Concentration field in a domain containing an interior layer with the width $H_l = 2.75$ m at times $t = 675$ (a), 1275 (b), 1950 (c), 3150 days (d).

the Fourier series to find the frequencies of periodic space structures. Let the function $f(x)$ be known. This function can be decomposed into the Fourier series according to the equation [15]

$$f(x) = \frac{1}{2}a_0 + \sum_{k=1}^{\infty} a_k \cos(k\omega x) + \sum_{k=1}^{\infty} b_k \sin(k\omega x) \quad (6)$$

The coefficients of the Fourier series a_0, a_k, b_k are defined as follows

$$\begin{aligned} a_0 &= \frac{2}{L} \int_{-L/2}^{L/2} f(\xi) d\xi, \quad a_k = \frac{2}{L} \int_{-L/2}^{L/2} f(\xi) \cos(k\omega\xi) d\xi, \\ b_k &= \frac{2}{L} \int_{-L/2}^{L/2} f(\xi) \sin(k\omega\xi) d\xi \end{aligned} \quad (7)$$

Here, $\omega = 2\pi/L$ with L to be the length of domain. We find the Fourier series coefficients for the functions $S_1(x)$ and $S_2(x)$ at different times being the same as in Fig. 4. The results are shown in Figs. 5 and 6. We see in Fig. 5 that the spectrum of $S_1(x)$ includes many different frequencies and high frequencies (corresponding to high k) are available. The number k is roughly equal to the number of repeating fragments, which form a periodic structure. Therefore, high frequencies are associated with small-scale space structures generated by the boundary layer near the upper boundary. However, at a long time, the coefficients of low frequency at $k \approx 4$ is dominant (Fig. 5 (d)) that is associated with the “brine ball” structure (Fig. 4(d)). The last one is induced by flows of pure water rising from the interior layer and being at low frequencies generated by this layer. As known, the average horizontal wavenumber is decreased with decreasing in the Rayleigh-Darcy number Rd . Therefore, the interior layer induces disturbances at lower horizontal wavenumber (at lower frequency) because of smaller Rd (due to the smaller magnitude of permeability). We see the interior layer starts to contribute to the spectrum in the space above from a certain time. The spectrum in the interior layer shows that high frequencies defined by motions above are damped in time (Fig. 6), that is the effect of flows coming from the top becomes less and less significant. On the contrary, coefficients at low k corresponding to its own low frequencies increase in time.

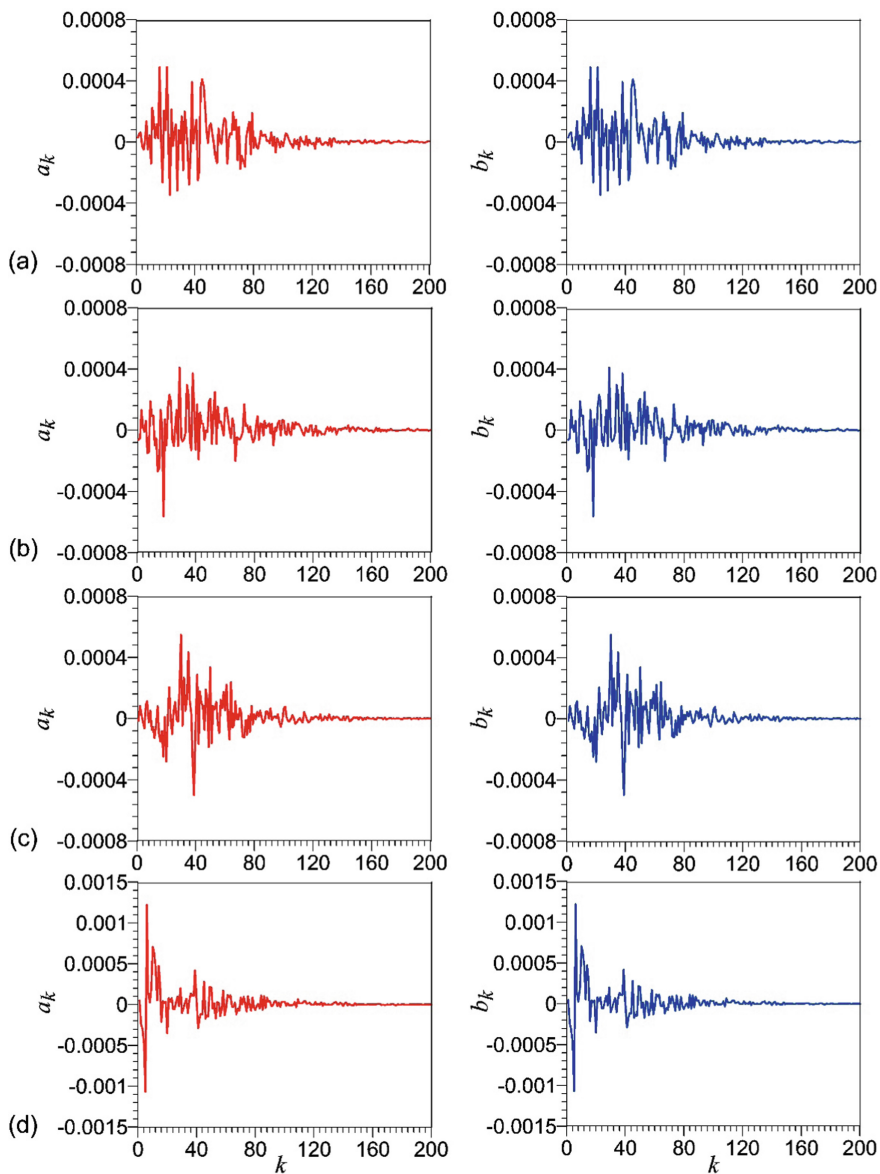


Fig. 5. Coefficients a_k (left) and b_k (right) of the Fourier series of the function $S_I(x)$ in the main medium at the level $y = -0.625$ m at times $t = 675$ (a), 1275 (b), 1950 (c), 3150 days (d).

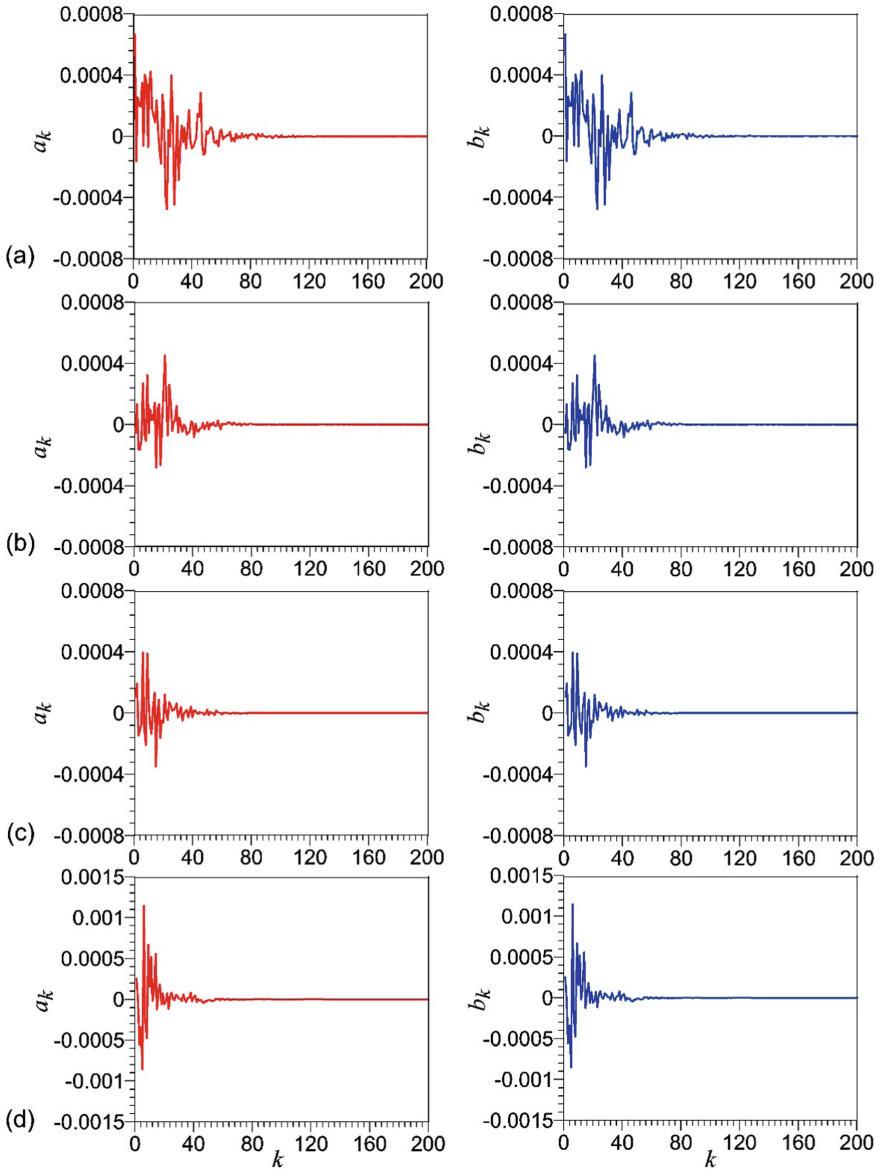


Fig. 6. Coefficients a_k (left) and b_k (right) of the Fourier series of the function $S_2(x)$ in the interior layer at the level $y = -2.50$ m at times $t = 675$ (a), 1275 (b), 1950 (c), 3150 days (d).

4 Conclusion

Stochastic haline convection in a rectangular porous domain containing a horizontal layer at lower porosity and permeability was investigated numerically. Convection is driven by more dense brine appearing near the upper boundary due to admixture diffusion and becoming unstable in the gravity field. As found, the interior layer is able to pass brine by different mode of convection. Initially, fluid here is involved in forced convection: the vertical component of velocity is directed downward or equal to zero. During time, the motion is rearranged and the upward velocity develops as well so forced convection transforms into natural convection. This dynamic stage is characterized by some fingers of pure water which rise from the layer to the space above and by flows intensified. Water fingers split brine between the upper boundary and interior layer into roughly periodic “brine balls”. An influence of layer on convection structure above is observed in this stage and our spectral analysis of density distributions confirms this conclusion.

Acknowledgments. The author would like to thank G.G. Tsyarkin for many fruitful discussions. This work has been supported by the Russian Science Foundation (grant № 16-11-10195).

References

1. Nield, D.A., Bejan, A.: *Convection in Porous Media*, 3rd edn. Springer, New York (2006)
2. Bear, J., Cheng, A.H.-D.: *Modeling Groundwater Flow and Contaminant Transport*. Springer, New York (2010)
3. Shargatov, V.A.: Instability of a liquid-vapor phase transition front in inhomogeneous wettable porous media. *Fluid Dyn.* **52**(1), 146–157 (2017). <https://doi.org/10.1134/S0015462817010148>
4. Tsyarkin, G.G.: Stability of the evaporation and condensation surfaces in a porous medium. *Fluid Dyn.* **52**(6), 777–785 (2017). <https://doi.org/10.1134/S0015462817060118>
5. Shargatov, V.A., Tsyarkin, G.G., Bogdanova, YuA: Filtration-flow fragmentation in medium with capillary-pressure gradient. *Dokl. Phys.* **63**(5), 199–2002 (2018). <https://doi.org/10.1134/S1028335818050038>
6. McKibbin, R.: Modeling heat and mass transport in geothermal systems. In: Vafai, K. (ed.) *Handbook of Porous Media*, chap. 7, pp. 545–572. Taylor & Francis, Boca Raton (2005)
7. Farajzadeh, R., Samili, H., Zitha, P.L.J., Bruining, H.: Numerical simulation of density-driven natural convection in porous media with application for CO₂ injection projects. *Int. J. Heat Mass Transf.* **50**, 5054–5064 (2007). <https://doi.org/10.1016/j.ijheatmasstransfer.2007.08.019>
8. Huppert, H.E., Neufeld, J.A.: The fluid mechanisms of carbone sequestration. *Ann. Rev. Fluid Mech.* **46**, 255–272 (2014). <https://doi.org/10.1146/annurev-fluid-011212-140627>
9. Anderson, L.: *New Theory of the Earth*. Cambridge University Press, Cambridge (2007)
10. Soboleva, E.: Numerical simulation of haline convection in geothermal reservoirs. *J. Phys.: Conf. Ser.* **891**, Paper 012105 (2017). <https://doi.org/10.1088/1742-6596/891/1/012105>
11. Soboleva, E.: Density-driven convection in an inhomogeneous geothermal reservoir. *Int. J. Heat Mass Transf.* **127**(C), 784–798 (2018). <https://doi.org/10.1016/j.ijheatmasstransfer.2018.08.019>

12. Soboleva, E.B., Tsypkin, G.G.: Numerical simulation of convective flows in a soil during evaporation of water containing a dissolved admixture. *Fluid Dyn.* **49**(5), 634–644 (2014). <https://doi.org/10.1134/S001546281405010X>
13. Soboleva, E.B., Tsypkin, G.G.: Regimes of haline convection during the evaporation of groundwater containing a dissolved admixture. *Fluid Dyn.* **51**(3), 364–371 (2016). <https://doi.org/10.1134/S001546281603008X>
14. Soboleva, E.: Numerical investigations of haline-convective flows of saline groundwater. *J. Phys.: Conf. Ser.* **891**, Paper 012104 (2017). <https://doi.org/10.1088/1742-6596/891/1/012104>
15. Korn, G.A., Korn, T.M.: *Mathematical Handbook for Scientists and Engineers: Definitions, Theorems, and Formulas for Reference and Review*, 2nd edn. McGraw-Hill Book Company, New York (1968)